Dyes and Pigments 107 (2014) 69–80

Contents lists available at ScienceDirect

Dyes and Pigments

journal homepage: www.elsevier.com/locate/dyepig

Synthesis of porphyrin glycoconjugates bearing thiourea, thiocarbamate and carbamate connecting groups: Influence of the linker on chemical and photophysical properties

Juliana C.C. Dallagnol [a], Diogo R.B. Ducatti [b], Sandra M.W. Barreira [a], Miguel D. Noseda [b], Maria Eugênia R. Duarte [b], Alan Guilherme Gonçalves [a,*]

[a] Departamento de Farmácia, Universidade Federal do Paraná, Av. Lothario Meissner, 3400, Jardim Botânico, Curitiba, Paraná, Brazil
[b] Departamento de Bioquímica, Universidade Federal da Paraná, Av. Cel. Francisco H. dos Santos, 100, Jardim das Américas, Curitiba, Paraná, Brazil

ARTICLE INFO

Article history:
Received 17 January 2014
Received in revised form
19 March 2014
Accepted 21 March 2014
Available online 29 March 2014

Keywords:
Porphyrins
Glycoporphyrins
Photostability
Photodynamic therapy
Singlet oxygen
Aggregation

ABSTRACT

In the present work, we have synthesized new porphyrin conjugates bearing thiourea, thiocarbamate and carbamate linkers using conventional and ultrasound-assisted methods. These molecules were synthesized by addition reactions using isothiocyanate derivates and amino- or hydroxyl-functionalized *meso*-tetra(aryl)porphyrins to give porphyrin analogs linked to glycosyl or benzyl moieties. Glycoporphyrin derivates could be obtained with better yields than their respective benzyl analogs. Thiourea and carbamate glycoporphyrins were also successfully synthesized through an ultrasound protocol with a remarkable decreasing of the reaction time. By NMR experiments we were able to evaluated the linker conformations which showed a preferred *Z,Z* conformation for the thiourea and carbamate derivatives. In addition, porphyrins were evaluated in terms of their UV–Vis spectra, singlet oxygen production, photostability and aggregation properties. Correlations between the linker type and the corresponding photophysical properties were observed. Carbamate porphyrins seem to be the most promising photosensitizers among the studied molecules due to their high singlet oxygen production, photostability and absence of self-assembling behavior in aqueous media.

1. Introduction

Since porphyrins have become part of the therapeutic arsenal for cancer treatment through photodynamic therapy (PDT), numerous studies have been dedicated to the synthesis of new and more efficient macrocyclic photosensitizers (PS). The first generation of PS is represented by hematoporphyrin derivates (e.g. Photofrin®), which gave place to a second generation that presented improved chemical homogeneity and radiation absorptivity at higher wavelengths of the visible spectrum [1–3]. However, both first and second generations of PS typically act as unspecific cytotoxic drugs. In this case, PDT selectivity towards the tumor tissue depends on the spatial focusing of the light source, as well as on the more active metabolism presented by malignant cells, which amplifies the photodamage promoted by the PS [4,5]. On the other hand, the lack of PS intrinsic selectivity can compromise the surrounding healthy tissue during PDT course. In this way, conjugation of PS to molecular moieties that can be selectively recognized by tumor cells have become of interest. Conjugated PS are then referred as the third generation of PS and their study currently represents an active research area [3,6].

A number of structural motifs based on biomolecules, such as proteins [7], immunoglobulins [8], cholesterol [9] and carbohydrates [10,11], have been chemically associated to macrocyclic rings in order to enhance the selectivity of PS uptake by the target cell. In this field, PS conceived through the attachment of glycosyl moieties to the porphyrin ring have proved to be promising candidates when targeted systems are desired [12]. This is related to the fact that cancer cells present higher amounts of lectins (carbohydrate binding proteins) on their surfaces than do regular cells [13,14]. Many porphyrin glycoconjugates have already been synthesized with ether [15,16], ester [17] or triazole [18,19] groups as linkers for binding the porphyrin to carbohydrate moieties. Nevertheless, these linkers could not be considered ideal because the deglycosylation process [20] as well as decreasing of biological activity [21] have already been reported as result of *in vitro* assays employing

* Corresponding author. Tel.: +55 41 3360 4065.
E-mail addresses: alan.goncalves@pq.cnpq.br, halagg@hotmail.com (A.G. Gonçalves).

http://dx.doi.org/10.1016/j.dyepig.2014.03.029
0143-7208/

those PS glycoconjugates. Thus, it is considered important to synthesize PS conjugates having different kinds of linkers in order to evaluate their chemical stability and their influence on photodynamic properties.

The formation of thiourea bridges is a well-known approach for binding different types of molecules through convergent synthesis. This kind of linkage was first utilized for the attachment of fluorescent probes to sensitive substrates, which could be performed under very mild conditions in the absence of catalysts [22]. Because of the versatility and robustness of this functional group, thiourea bridges became a common linker for binding carriers to biologically active molecules. However, there are only a few examples of the synthesis of porphyrins bearing thiourea linkers. Clark and Boyle (1999) [23] synthesized thiourea-containing porphyrins by using isothiocyanate-functionalized porphyrins and a series of amino compounds, including amino acids, aliphatic and aromatic amines as starting materials. Other related studies made use of reactions employing amino porphyrins and isothiocyanate compounds [24]. Thiourea-related linkers, such as thiocarbamate and carbamate groups, have also facile synthesis methodologies; nevertheless they are poorly explored for the synthesis of conjugated porphyrins. Although the thiocarbamate linker can be promptly obtained from reactions of hydroxyl compounds with isothiocyanate derivates, to the best of our knowledge there is no example of this kind of linkage involving porphyrin synthesis. This fact could be related to the previously noted instability of the thiocarbamate bridge [25,26]. There are two reported examples of carbamate-linked porphyrins where hydroxy-porphyrins and isocyanate-functionalized compounds were utilized as starting materials [27,28]. The above cited linkers have never been previously used for functionalizing porphyrins with carbohydrate moieties. Also, a comparative evaluation of the influence of such linkers on porphyrin photophysical properties is yet to be performed. PS photophysical evaluation is considered key in order to understand, or even predict, porphyrin photodynamic potentialities [29].

Here, we have investigated the synthesis of porphyrin conjugates bearing thiourea, thiocarbamate and carbamate linkers. For this purpose, we utilized amino- or hydroxy-functionalized *meso*-tetra(aryl)porphyrins and per-*O*-acetyl-β-D-glucopyranosyl isothiocyanate as starting materials. We have also employed benzyl isothiocyanate in order to obtain non-glycosyl porphyrin conjugate analogs for intercomparison of their properties. The linker conformation of the porphyrin conjugates was evaluated by NMR spectroscopy. Due to the potential interest in this class of compounds in PDT, photophysical and physicochemical properties of those conjugates were studied, including determination of singlet oxygen production and photostability, evaluation of the electronic spectra and aggregation studies.

2. Material and methods

2.1. General procedures

The ^{1}H NMR, ^{13}C NMR and 2D experiments (HMBC-^{1}H/^{13}, NOESY ^{1}H/^{1}H) were obtained with a Bruker AVANCE III 400 spectrometer with the indicated solvents operating at 400.15 MHz and 100.62 MHz respectively. Chemical shifts (δ) are expressed in parts per million (ppm) and coupling constants (J) in Hertz (Hz) using residual solvent peaks as internal standards. Low resolution mass spectra were obtained with a Bruker MALDI-TOF spectrometer with HCCA matrix. The high resolution mass spectra (HRMS) were recorded with two different spectrometers: (a) a Bruker MicroTOF-Q II XL operating in the positive-ion mode with porphyrins at 100 μg mL^{-1} in methanol using sodium formate solution as reference or (b) a Bruker LTQ Orbitrap operating in the positive-ion mode with porphyrins at 10 μg mL^{-1} in methanol using Ultramark 1621 as reference. Optical rotation values were obtained with a Jasco P-200 polarimeter equipped with a sodium light source from 1% (g 100 mL^{-1}) porphyrin solutions in DMSO. UV–Vis spectra were recorded with a Shimadzu UV-1800 spectrometer using porphyrin concentration at 12 μmol L^{-1} in chloroform. Fluorescence emission spectra were recorded with an RF-5301PC Shimadzu spectrofluorometer using porphyrin concentrations as indicated in Fig. 8 and chloroform as solvent. Infrared (IR) experiments were performed with KBr in an FTIR Bomen/MB analyzer. The light source used for the photophysical assays was a Lumacare LC 122A with a halogen/quartz 250 W lamp. All compounds were stored at 5 °C in a 1 mmol L^{-1} DMSO solution (stock solutions) before the photophysical assays. These experiments were conducted at room temperature in a dark room to avoid any impact of ambient light over the main light source. Compounds **9** and **11** were analyzed just after purification with less than 24 h storing.

2.2. Synthesis and purification

Reagents and solvents were of reagent grade. For anhydrous reactions, the solvents were dried according to stated methods [30]. Acetonitrile was dried by soaking it with silica gel for 24 h followed by distillation. DMF was dried by soaking it for 24 h with anhydrous $MgSO_4$. The dried solvents were then stored in flasks containing molecular sieves 4 Å under nitrogen atmosphere. Column chromatography was performed with the indicated solvents using Sigma silica gel 60 (particle size 220–440 mesh). Yields refer to chromatographically and spectroscopically pure compounds. Compounds **1** [31], **2** [32], **3** [31], **4** [33], **5** [34] and **6** [35] are known compounds and their spectroscopic data coincided to those reported previously (for spectroscopy data see Supplementary Information).

2.2.1. Synthesis of 5-[4-((2′,3′,4′,6′-tetra-O-acetyl-β-D-glucopyranosyl)thioureido)-phenyl]-10,15,20-triphenylporphyrin (**7**)

Method A: 5-(4-aminophenyl)-10,15,20-triphenylporphyrin **3** (63 mg 0.1 mmol) and per-*O*-acetyl-β-D-glucosyl isothiocyanate **5** (78 mg, 0.2 mmol) were dissolved in chloroform (4 mL) and stirred under reflux for 24 h. The resulting mixture was concentrated under vacuum and the residue was purified by silica gel column using chloroform/methanol (99:1) as mobile phase to give **7** as a purple solid (73 mg, 72% yield). Method B: **3** (63 mg 0.1 mmol) and **5** (78 mg, 0.2 mmol) were dissolved in chloroform (4 mL) and placed in an ultrasonic bath (42 MHz) for 1 h at room temperature. The resulting mixture was concentrated under reduced pressure and the residue was chromatographed as outlined for Method A, giving **7** with 69% yield (70 mg).

$[a]_D^{25}$ + 6.25 (*c* 1.0, DMSO); **^{1}H NMR** (400 MHz, DMSO-d_6) δ (ppm) 10.35 (s, 1H, N–H linker); 8.92 (d, J = 4.3 Hz, 2H, β-pyrrole), 8.83 (m, 6H, β-pyrrole); 8.50 (d, $J_{HN\text{-}H1'}$ = 8.5 Hz, 1H, N′-H linker), 8.21 (d, J = 5.6 Hz, 6H, *o*-phenyl); 8.18 (d, J = 8.4 Hz; 2H, *o*-phenyl linker); 7.96 (d, J = 8.4 Hz; 2H, *m*-phenyl linker); 7.84 (m, 9H, *m*- and *p*-phenyl); 6.04 (t, $J_{H1'\text{-}HN}$ = 8.5 Hz, 1H, H-1′); 5.45 (t, 1H, $J_{H2'\text{-}H3'}$ = 9.5 Hz, 1H, H-3′); 5.15 (t, $J_{H2'\text{-}H3'}$ = 9.5 Hz, 1H, H-2′); 5.03 (t, $J_{H4'\text{-}H5'}$ = 9.7 Hz, 1H, H-4′); 4.27–4.13 (m, 2H, H-5′ e H-6a′); 4.07 (m, $J_{6a\text{-}6b}$ = 12.0 Hz, H-6b′); 2.09–1.99 (4s, 12H, CH_3); −2.89 (s, NH-pyrrole). **^{13}C NMR** (101 MHz, DMSO-d_6) δ (ppm)181.9 (C=S); 170.1; 169.9; 169.6; 169.4 (4C, C=O); 141.2; 138.7; 137.5; 135.2; 134.5; 131.4; 128.1; 127.0; 121.5; 120.0; 119.6 (44C, tetraarylporphyrin); 81.4; 72.9; 72.3, 70.6; 68.0; 61.8 (6C, sugar moiety); 20.6; 20.5; 20.4; 20.3 (4C, CH_3).UV–Vis ($CHCl_3$) λ_{max} (log ε) 419 (5.38), 516 (4.04), 551 (3.70), 590 (3.52), 646 (3.38) nm. IR (KBr):

ν_{max} 3315, 1751, 1704, 1515, 1222 cm^{-1}. HRMS: *m/z* calc. for $[M+H]^+$, $C_{59}H_{51}N_6O_9S^+$: 1019.3433; found: 1019.3433.

2.2.2. Synthesis of 5-[4-((methylbenzene)thioureido)-phenyl]-10,15,20-triphenylporphyrin (*8*)

5-(4-Aminophenyl)-10,15,20-triphenylporphyrin **3** (63 mg 0.1 mmol) and benzyl isothiocyanate **6** (150 mg, 1.0 mmol) were dissolved in chloroform (4 mL) and stirred under reflux for 24 h. The resulting mixture was dried under vacuum and the resulting residue was chromatographed on a silica gel column with ethyl acetate/hexanes (1:1) as mobile phase (40 mg, 52% yield).

^{1}H NMR (400 MHz, DMSO-d_6) δ (ppm) 10.06 (s, 1H, N–H linker); 8.93 (d, J = 4.3 Hz, 2H, β-pyrrole), 8.83 (m, 6H, β-pyrrole); 8.53 (t, $J_{NH\text{-}CH2}$ = 5.3 Hz, 1H, N′–H linker), 8.20 (m, 6H, *o*-phenyl); 8.17 (d, J = 8.3 Hz; 2H, *o*-phenyl linker); 7.97 (d, J = 8.3 Hz; 2H, *m*-phenyl linker); 7.81 (m, 9H, *m*- and *p*-phenyl); 7.46 (d, $J_{o\text{-}m}$ = 7.3 Hz, 2H, o-benzyl); 7.40 (t, $J_{m\text{-}p}$ = 7.5 Hz, 2H, m-benzyl); 7.30 (t, $J_{m\text{-}p}$ = 7.5 Hz, 1H, p-benzyl); 4.90 (d, $J_{NH\text{-}CH2}$ = 5.3 Hz, 2H, CH_2); −2.87 (s, NH-pyrrole). **^{13}C NMR** (101 MHz, DMSO-d_6) δ (ppm) 181.0 (C=S); 141.2; 139.4; 139.0; 136.7; 134.6; 131.4; 128.4; 128.1; 127.5; 127.0; 121.0; 120.0; 119.96; 119.90 (50C, tetraarylporphyrin and aromatic benzyl); 47.3 (CH_2). UV–Vis ($CHCl_3$) λ_{max} (log ε) 420 (5.24), 516 (3.84), 551 (3.51), 590 (3.51), 646 (3.18), 710 (2.62) nm. IR (KBr): ν_{max} 3315, 1701, 1517 cm^{-1}. HRMS: *m/z* calc. for $[M+H]^+$, $C_{52}H_{39}N_6S^+$: 779.2951 found: 779.2952.

2.2.3. Synthesis of 5-[phenoxy-4-thiocarbonyl-(1′-deoxyamino-2′,3′,4′,6′-tetra-O-acetyl-β-D-glucopyranosyl)]-10,15,20-triphenylporphyrin (*9*)

5-(4-Hydroxyphenyl)-10,15,20-triphenylporphyrin **4** (63 mg 0.1 mmol), glucosyl isothiocyanate **5** (78 mg, 0.2 mmol) and triethylamine (3 μL, 0.02 mmol) were dissolved in chloroform (4 mL) and stirred under reflux for 48 h. The resulting mixture was dried under reduced pressure and the residue was chromatographed on a column of silica gel (10 × 500 mm) with chloroform/ethyl acetate (40:1) as mobile phase. The first fraction eluted (Rf = 0.44) was the desired product (**9**, 23 mg, 23% yield).

$[a]_D^{25}$ + 4.31 (*c* 1.0, DMSO); **^{1}H NMR** (600 MHz, DMSO-d_6) δ (ppm) 10.82 and 10.59 (2d, $J_{HN\text{-}H1}$ = 9.0 and 8.6 Hz, respectively, 1H, N–H linker), 8.83 (m, 8H, β-pyrrole); 8.24 (d, J = 8.2 Hz; 2H, *o*-phenyl linker), 8.21 (d, 6H, *o*-phenyl); 7.82 (d, 9H, *m*- and *p*-phenyl); 7.51 (d, $J_{o\text{-}m}$ = 8.2 Hz; 2H, *m*-phenyl linker); 5.97 and 5.93 (2t, $J_{HN\text{-}H1}$ = 9.0 and 8.6 Hz, respectively, 1H, H-1′); 5.51 (t, 1H, H-3′); 5.16 (t, 1H, H-2′); 5.01 (t, 1H, H-4′); 4.26 (m, 2H, H-5′ and H-6a'), 4.11 (m, 1H, H-6b′); 2.09; 2.06; 2.04; 2.00 (4s, 12H, CH_3); −2.87 (s, NH-pyrrole). **^{13}C NMR** (101 MHz, DMSO-d_6) δ (ppm) 183.1 (C=S); 170.5; 169.9; 169.6; 169.5 (4C, C=O); 153.3; 141.6; 141.5; 135.4; 134.7; 131.9; 128.6; 127.4; 121.8; 120.6; 119.5 (44C, tetraarylporphyrin); 82.7; 73.2; 72.0, 71.8; 68.0; 62.0 (6C, sugar moiety); 20.9; 20.8; 20.7; 20.67 (4C, CH_3). UV–Vis ($CHCl_3$) λ_{max} (log ε) 419 (5.34), 516 (3.93), 552 (3.65), 591 (3.41), 646 (3.26) nm. HRMS: *m/z* calc. for $[M+H]^+$, $C_{59}H_{50}N_5O_{10}S^+$: 1020.3273; found: 1020.3292.

2.2.4. Synthesis of 5-[phenoxy-4-carbonyl-(1′-deoxyamino-2′,3′,4′,6′-tetra-O-acetyl-β-D-glucopyranosyl)]-10,15,20-triphenylporphyrin (*10*)

Method A: 5-(4-hydroxyphenyl)-10,15,20-triphenylporphyrin **4** (63 mg 0.1 mmol), glucosyl isothiocyanate **5** (78 mg, 0.2 mmol) and triethylamine (3 μL, 0.02 mmol) were dissolved in chloroform (4 mL) and stirred under reflux for 24 h. NaOH (4 mg, 0.1 mmol) was then added to the reaction flask and the resulting mixture was kept for additional 24 h under stirring at room temperature. Reaction was concentrated under vacuum and the residue was chromatographed on a silica gel column with chloroform/ethyl acetate (40:1) as mobile phase. The second chromatographic fraction eluted was the desired product **10** (Rf = 0.37) with 49% yield (49 mg). Method B: **4** (63 mg 0.1 mmol), **5** (78 mg, 0.2 mmol) and triethylamine (3 μL, 0.02 mmol) were dissolved in chloroform (4 mL) and placed in an ultrasonic bath (42 MHz) for 1 h at room temperature. The resulting mixture was dried under reduced pressure and the residue chromatographed as described for Method A (**10**, 40 mg, 40% yield).

$[a]_D^{25}$ + 5.85 (*c* 1.0, DMSO); **^{1}H NMR** (400 MHz, DMSO-d_6) δ (ppm) 9.97 (br, 1H, N–H linker); 8.92 (d, J = 4.6 Hz, 2H, β-pyrrole), 8.82 (m, 6H, β-pyrrole); 8.22 (d, 6H, *o*-phenyl); 8.02 (d, $J_{o\text{-}m}$ = 8.4 Hz; 2H, *o*-phenyl linker); 7.84 (m, 9H, *m*- and *p*-phenyl); 7.22 (d, J = 8.4 Hz; 2H, *m*-phenyl linker); 5.61 (d, $J_{H1\text{-}H2}$ = 8.7 Hz, 1H, H-1′); 5.34 (t, 1H, $J_{H2\text{-}H3}$ = 9.6 Hz, 1H, H-3′); 5.01 (m, 2H, H-2′ and H-4′); 4.13 (m, 2H, H-5′ e H-6a'); 4.05 (d, $J_{6a\text{-}6b}$ = 11.8 Hz, H-6b′), 2.08–1.97 (4s, 12H, CH_3); −2.87 (s, NH-pyrrole). **^{13}C NMR** (101 MHz, DMSO-d_6) δ (ppm) 166.9; 166.4; 166.1; 165.9 (4C, C=O); 154.4 (C=O, linker) 138.2; 137.9; 132.5; 131.1; 128.4; 125.0; 123.9; 117.6; 116.8; 116.6; 110.9 (44C, tetraarylporphyrin); 79.2; 69.8; 68.5; 68.3; 64.5; 58.5 (6C, sugar moiety); 17.4; 17.36; 17.31; 17.2 (4C, CH_3). UV–Vis ($CHCl_3$) λ_{max} (log ε) 419 (5.37), 516 (3.98), 552 (3.67), 590 (3.45), 646 (3.34) nm. IR (KBr): ν_{max} 3315, 1751, 1222 cm^{-1}. HRMS: *m/z* calc. for $[M+H]^+$, $C_{59}H_{50}N_5O_{11}^+$: 1004.3501; found: 1004.3457.

2.2.5. Synthesis of 5-(phenoxy-4-thiocarbonyl-aminomethylbenzene)-10,15,20-triphenylporphyrin (*11*)

5-(4-Hydroxyphenyl)-10,15,20-triphenylporphyrin **4** (63 mg 0.1 mmol), benzyl isothiocyanate **6** (150 mg, 1.0 mmol) and triethylamine (3 μL, 0.02 mmol) were dissolved in chloroform (4 mL) and stirred under reflux for 48 h. The resulting mixture was dried under reduced pressure and the residue was chromatographed on silica gel column with chloroform as mobile phase. The first chromatographic fraction eluted (Rf = 0.70) gave **11** with 20% yield (16 mg).

^{1}H NMR (400 MHz, DMSO-d_6) δ (ppm) 10.55 and 10.34 (2t, $J_{HN\text{-}CH2}$ = 5.9 and 6.2 Hz, respectively, 1H, N–H linker); 8.84 (m, 8H, β-pyrrole); 8.21 (m, 8H, *o*-phenyl); 7.82 (m, 9H, *m*- and *p*-phenyl); 7.52 (d, $J_{o\text{-}m}$ = 8.4 Hz); 7.46 (m, 2H, *o*-benzyl); 7.41 (t, $J_{m\text{-}p}$ = 7.7 Hz, 2H, *m*-benzyl); 7.33 (t, $J_{m\text{-}p}$ = 7.7 Hz, 1H, *p*-benzyl); 4.87 and 4.71 (2d, $J_{HN\text{-}CH2}$ = 5.9 and 6.2 Hz, respectively, 2H, CH_2); −2.89 (s, 2H, NH-pyrrole). **^{13}C NMR** (101 MHz, DMSO-d_6) δ (ppm) 189.3 (C=S); 153.3; 141.2; 138.5; 137.6; 134.9; 134.2; 131.6; 128.5; 128.1; 127.6; 127.4; 127.0; 121.4; 120.1; 119.2; (50C, tetraarylporphyrin and aromatic benzyl); 48.7 (CH_2). UV–Vis ($CHCl_3$) λ_{max} (log ε) 419 (5.40), 515 (4.08), 551 (3.73), 590 (3.56), 645 (3.43) nm. HRMS: *m/z* calc. for $[M+H]^+$, $C_{52}H_{38}N_5OS^+$: 780.2792; found: 780.2841.

2.2.6. Synthesis of 5-(phenoxy-4-carbonyl-aminomethylbenzene)-10,15,20-triphenylporphyrin (*12*)

5-(4-Hydroxyphenyl)-10,15,20-triphenylporphyrin **4** (63 mg 0.1 mmol) benzyl isothiocyanate **6** (150 mg, 1.0 mmol) and triethylamine (3 μL, 0.02 mmol) were dissolved in chloroform (4 mL) and stirred under reflux for 24 h. NaOH (4 mg, 0.1 mmol) was then added to the reaction flask and resulting mixture was kept for additional 24 h under stirring at room temperature. The resulting mixture was dried under reduced pressure and the residue was applied to a silica gel column with chloroform as mobile phase. Chromatography gave only one fraction (Rf = 0.59), which was the desired product (**12**) with 32% yield (24 mg).

^{1}H NMR (600 MHz, DMSO-d_6) δ (ppm) 8.83 (m, 8H, β-pyrrole); 8.57 (t, $J_{NH\text{-}CH2}$ = 6.1 Hz, 1H, N–H linker); 8.20 (m, 8H, *o*-phenyl); 7.82 (m, 9H, *m*- e *p*-phenyl); 7.56 (d, $J_{o\text{-}m}$ = 8.4 Hz, 2H, *m*-phenyl linker); 7.43 (m, 4H, *m*- and *o*-benzyl); 7.31 (t, $J_{m\text{-}p}$ = 7.0 Hz, 1H, *p*-benzyl); 4.41 (d, $J_{HN\text{-}CH2}$ = 6.1 Hz, 2H, CH_2); −2.91 (s, NH-pyrrole). **^{13}C NMR** (101 MHz, DMSO-d_6) δ (ppm) 154.8 (C=O); 151.2; 141.2; 139.3; 137.8; 135.0; 134.2; 128.5; 128.1; 127.3; 127.0; 120.2; 120.1; 119.3; (50C, tetraarylporphyrin and aromatic benzyl); 44.3 (CH_2).

UV–Vis ($CHCl_3$) λ_{max} (log ε) 419 (5.40), 515 (4.06), 550 (3.68), 590 (3.52), 645 (3.35) nm. IR (KBr): ν_{max} 3317, 1730, 1207 cm^{-1}. HRMS: *m*/*z* calc. for $[M+H]^+$, $C_{52}H_{38}N_5O_2^+$: 764.3020 found: 764.3033.

2.3. Singlet oxygen measurements

Singlet oxygen production was estimated through the indirect method described by Roitman and co-workers [36] with modifications. Freshly prepared solutions of 1,3-diphenylisobenzofuran (DPBF) (50 μmol L^{-1}) and the tested porphyrin (0.5 μmol L^{-1}, prepared from the stock solutions) in DMF:H_2O (9:1) were irradiated with 9.0 mW/cm^2 with a Lumacare light source using a yellow filter (550–800 nm) at room temperature, under stirring for different periods of time (from 0 to 30 min; see Fig. 4). The same procedure was performed for the standard photosensitizer, methylene blue (MB). The reaction of DPBF with $^1O_2$ was monitored by the reduction of intensity of the absorption band at 415 nm over time. The absorbance values were measured twice in independent experiments and the results were expressed in percentage with the corresponding standard deviation. The singlet oxygen quantum yields were obtained from Equation (1) using just the first eight minutes, which corresponded to range of time that presented a linear relationship with the natural logarithm (ln) of the DPBF absorbance.

$$\Phi_\Delta = \Phi_\Delta^{Std}\frac{R\cdot I_{abs}^{Std}}{R^{Std}\cdot I_{abs}} \quad (1)$$

In Equation (1), Φ_Δ represents the oxygen singlet yield of the sample, with Φ_Δ^{Std} being the standard quantum yield (for MB, 0.52).

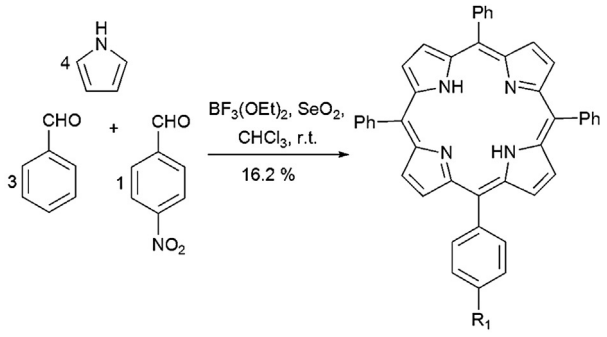

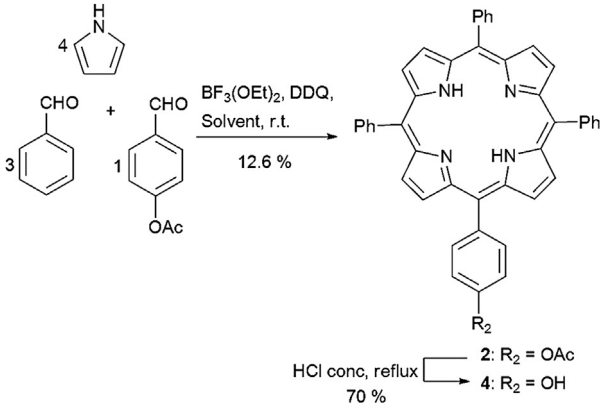

Scheme 1. Synthesis of mono-substituted amino and hydroxyl meso-tetra(aryl) porphyrins **3** and **4**.

Table 1
Optimization of the reaction conditions for the synthesis of thiourea glycoporphyrin **7**.

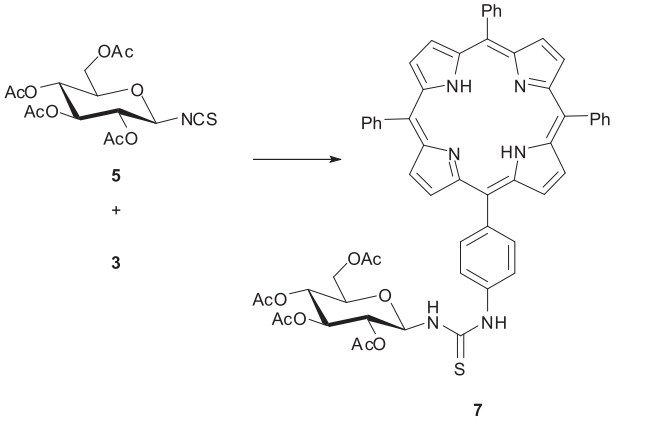

Entry	5 (equiv)	Time (h)	*T* (°C)	Et_3N (equiv)	Yield (%) 7[b]
1[a]	2	4	r.t.	–	10
2[a]	10	4	r.t.	–	15
3[a]	2	24	r.t.	–	54
4[a]	2	24	Reflux	–	72
5[a]	2	48	Reflux	–	70
6[a]	2	48	Reflux	0.2	60[c]
7[d]	2	1	Reflux	–	69

[a] Reactions performed with 3 (0.1 mmol), in 2 mL of $CHCl_3$.
[b] Yields estimated from flash chromatography.
[c] Traces of glycoporphyrin bearing an urea group were detected.
[d] Reaction performed with 3 (0.1 mmol), in 2 mL of $CHCl_3$, ultrasound (42 MHz).

R and R^{Std} are the rate constants of DPBF consumption in the presence of porphyrins and MB, respectively. Since it is a first order reaction, these parameters were obtained from a plot of the ln of DPBF consumption. I_{abs} and I_{abs}^{Std} are the rates of light absorption for the sample and the standard, respectively [29].

2.4. Photostability studies

The photostability evaluation was performed by Gomes and coworkers method [37]. Aqueous solutions of porphyrin (10 μmol L^{-1}, prepared from the stock solutions) were irradiated with 100 mW/cm^2 using Lumacare light source at room temperature under stirring for different periods of time (from 0 to 30 min, see Fig. 6). To avoid porphyrin aggregation, **7** and **9** were dissolved in an SDS solution (0.1 mg %). The results were monitored in terms of the

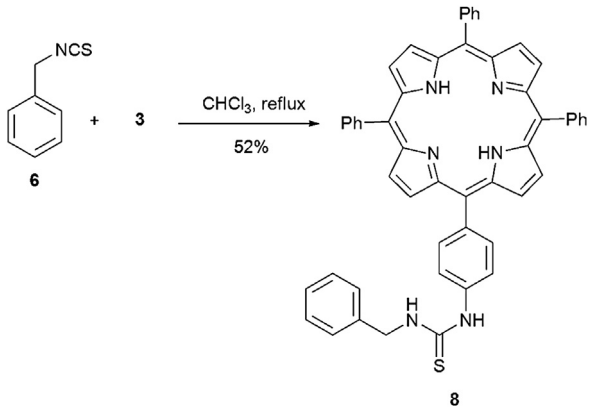

Scheme 2. Synthesis of thiourea benzyl-porphyrin **8**.

reduction of Soret band absorption intensity over time. The extinction of Soret band was measured twice with independent experiments and the results were expressed in percentage with the correspondent standard deviation.

2.5. Aggregation studies

Aqueous solutions of the porphyrins in different concentrations were prepared from the stock solutions, as indicated in Figs. 7 and 8. Solutions were then measured by means of UV–Vis absorption and fluorescence emission. As previously described [38], porphyrin self-assembling behavior was evaluated through the observation maximum absorbance or emission shifting in function of the porphyrin concentration.

3. Results and discussion

3.1. Chemistry

In the present work, the synthesis of porphyrin conjugates was planned based on the use of isothiocyanate derivatives and asymmetric *meso*-tetra(aryl)porphyrins containing one amino or hydroxyl group. To synthesize the mono-substituted porphyrins, we decided to make a brief study on different synthetic routes aiming to better overall yields. This study was performed by reproducing some literature porphyrin synthesis [39–42] and by slightly modifying established methodologies [31,40,43] (for details see Supplementary Information). The best overall yield for amino-tetra(aryl)porphyrin **3** synthesis was achieved via the corresponding nitro-tetra(aryl)porphyrin **1** route. For this purpose, we first performed a cyclocondensation reaction of pyrrole, benzaldehyde and *p*-nitrobenzaldehyde followed by porphyrinogen oxidation with SeO_2, an oxidizing agent that has been recently introduced by us for porphyrin synthesis [40]. Nitro compound **1** was then reduced to amine **3** using Sn^0 as reducing agent under acid conditions (Scheme 1). The route selected for the synthesis of hydroxy-tetra(aryl)porphyrin **4** involved aqueous acid hydrolysis of acetoxy-tetra(aryl)porphyrin **2**. In contrast to porphyrin **1** synthesis, compound **2** best yield was achieved in conditions having DDQ (2,3-dichloro-5,6-dicyano-1,4-benzoquinone), instead of SeO_2, as oxidizing agent (Scheme 1).

Diverse approaches have been reported for the preparation of glycosyl isothiocyanate building blocks [44–46]. Here, compound **5** was synthesized from acetobromoglucose through bromide nucleophilic displacement with KSCN [34]. Having both glycosyl isothiocyanate and porphyrin starting materials, we initiated an optimization study with **5** and porphyrin **3** to prepare the thiourea glycoporphyrin **7** (Table 1). Product (**7**) structure was confirmed unambiguously by the expected spectral features, including the deshielded position of C=S signal in the ^{13}C NMR spectra at 181.9 ppm. Reaction conditions using room temperature for four hours (Table 1, entry 1) gave **7** in low yield (10%). Even utilizing increased amounts of the isothyocyanate **5**, no important yield enhancement was achieved (entry 2). We then decided to use longer reactions times, as well as a higher temperature (entries 3–5). The resulting conditions improved the reaction outcome and glycoporphyrin **7** was obtained with 72% yield by using 24 h reaction under reflux (entry 4). A condition attempting the using of Et_3N as catalyst showed an acceptable yield (entry 6); however, traces of a porphyrin glycoconjugate bearing a urea group was identified by mass spectroscopy analysis (see Supplementary Information). With the objective of reducing the reaction time, we submitted a reaction mixture identical as that outlined for entry 4 to ultrasound irradiation under room temperature (entry 7). To our delight, the reaction time was reduced to 1 h with no substantial decreasing in reaction yield.

As one of our main objectives was to understand the effect of the linker on the physicochemical and photophysical properties of the resulting porphyrin conjugates, we attempted to discriminate the influence of the carbohydrate moiety on such properties. For this purpose, we also synthesized a non-glycosyl thiourea porphyrin conjugate. Specifically, we prepared benzyl isothiocyanate **6** from benzyl bromide [47], which was in turn submitted to the optimized protocol with amino-tetra(aryl)porphyrin **3** (conditions identical as indicated in entry 4 of Table 1, except for the addition of 10 equiv. of benzyl isothiocyanate **6**) for the synthesis of hitherto unreported porphyrin **8** (Scheme 2). Attempts to reduce the reaction time using ultrasound were unsuccessful, and just traces of target porphyrin **8** were detected.

Table 2
Reaction conditions for the synthesis of thiocarbamate **9** and carbamate **10** glycoporphyrins.

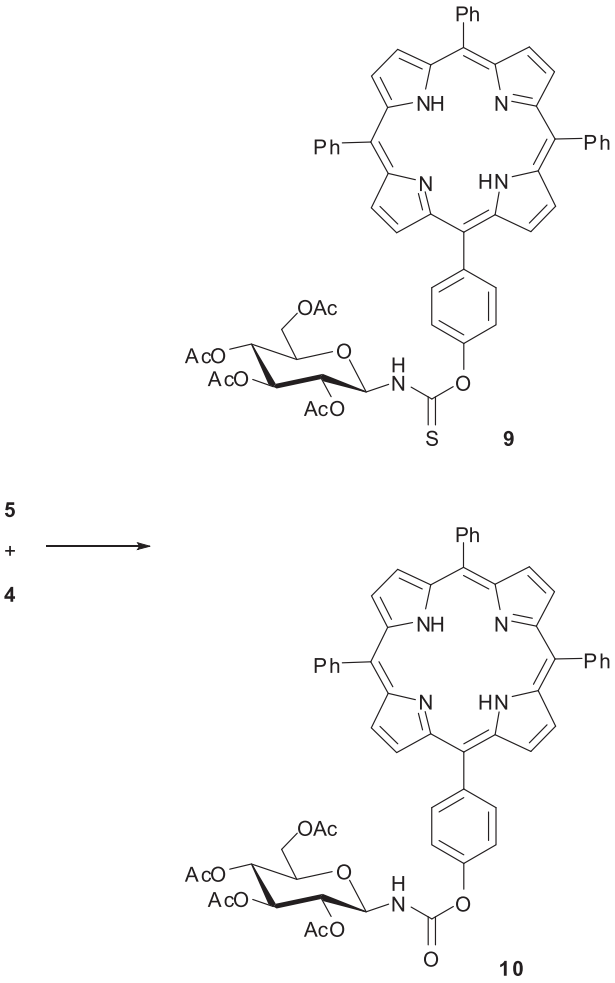

Entry	5 (equiv)	Time (h)	*T* (°C)	Et_3N (equiv)	Yield (%) 9/10[b]
1[a]	2	48	Reflux	–	19/–
2[a]	2	48	Reflux	0.2	23/33
3[c]	2	1	r.t.	0.2	8/40
4[d]	2	48	Reflux	0.2	–/49

[a] Reactions performed with 4 (0.1 mmol), in 2 mL of $CHCl_3$.
[b] Yields estimated from flash chromatography.
[c] Reaction performed with 4 (0.1 mmol), in 2 mL of $CHCl_3$, ultrasound (42 MHz).
[d] Reactions performed with 4 (0.1 mmol), in 2 mL of $CHCl_3$. Then NaOH (1 equiv) was added for 24 h under room temperature.

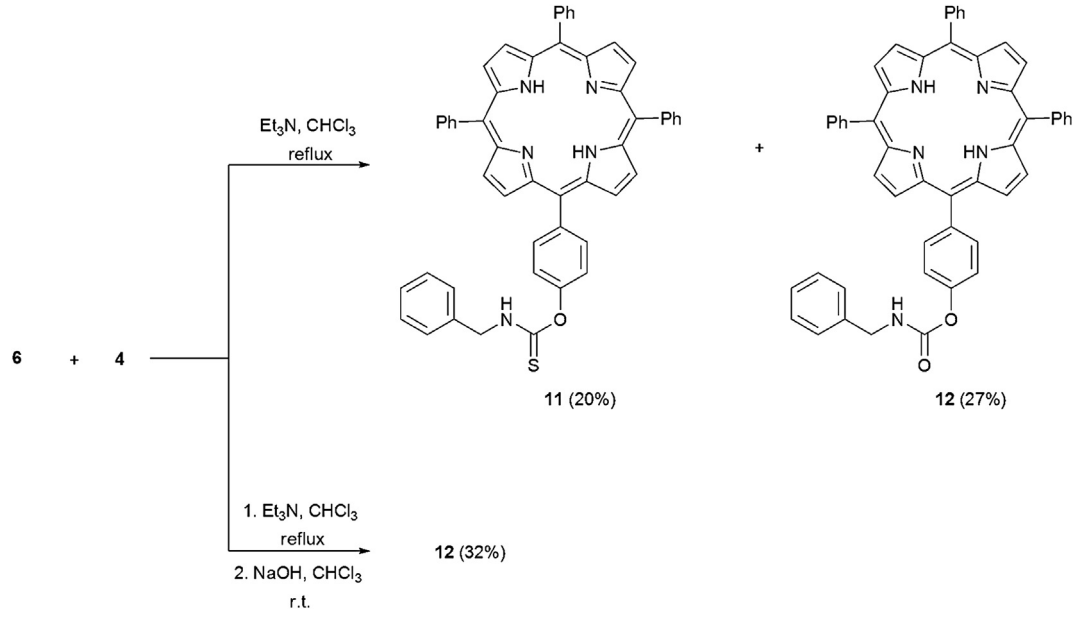

Scheme 3. Synthesis of thiocarbamate (**11**) and carbamate (**12**) benzyl-porphyrins.

Addition reactions of hydroxyl compounds to *O*-protected glycosyl isothiocyanates have been often reported for the synthesis of thiocarbamate glycoconjugates [48,49]. Due to the lower nucleophilicity of hydroxyl in relation to amino groups, some protocols have been optimized with bases as catalysts to perform such reactions [50]. However, carbamate derivatives have been produced as byproducts under those conditions [51]. Notwithstanding this observation, the sulfur–oxygen exchange related to thiocarbamates can be synthetically useful. This is based on the fact that the obvious starting materials for carbamate synthesis (isocyanates) rapidly subside to hydrolysis upon exposure to moisture. Because isothiocyanate compounds are easier to handle [23], their employment as starting materials for the synthesis of carbamates have been recently explored [52]. In the present work, we exercised reaction versatility by synthesizing both porphyrin thiocarbamate **9** and porphyrin carbamate **10** from hydroxy-tetra(aryl)porphyrin **4** and glycoside **5** (Table 2). We first applied the protocol that proved to be the most efficient based on the synthesis of the thiourea compounds **7** and **8** to give thiocarbamate **9** with 19% yield (Table 2, entry 1). The base catalyzed reaction shown in entry 2 (Table 2) also produced **9**, although in lower yield in relation to carbamate porphyrin **10**. The linker structure could be discriminated for both products by ^{13}C NMR spectroscopy. In agreement with literature data [28,53,54], the C═S carbon of **9** was assigned at 183.1 ppm and the C═O carbon of **10** at 154.4 ppm. Reaction using ultrasound irradiation under room temperature (entry 3) gave mainly the carbamate porphyrin **10** at a reduced reaction time (1 h). At this stage, we planned a protocol to exclusively obtain the carbamate derivative **10**, which was developed by adding NaOH and keeping the resulting reaction mixture for 24 h at room temperature (entry 4).

With the above information to hand, the synthesis of benzyl thiocarbamate and carbamate porphyrins **11** and **12** were performed as shown in the Scheme 3. Attempts to reduce reaction time using ultrasound were unsuccessful, and just traces of target porphyrins **11** and **12** were found. Considering the fact that the ultrasound-assisted reactions only gave good results for the synthesis of the glycoporphyrins, we concluded that the type of the isothycianate utilized as starting material seemed to have a pivotal importance for the success of the ultrasound protocol.

Evaluation of the ^{1}H NMR spectra of compounds **7**–**12** was conducted considering the fact that thiourea, thiocarbamate and carbamate units are not rigid linkers, but they can experience a reduction of the rotation of the C–N pseudo-amide bond [55–57]. For this reason, these compounds could generate NMR spectra consistent with the presence of distinct populations of conformers. According to the literature [26] due to the greater bulk and polarizability of sulfur in comparison to oxygen, the rotational energetic barrier is typically higher for *N*-thiocarbonyls than for the carbonyl analogs. When comparing the *N*-thiocarbonyl counterparts, the energy related to the rotation of the *N*-group out of the plane is usually higher for thiocarbamate than for thiourea. Here, ^{1}H NMR spectra of each of the thiourea compounds **7** and **8** gave only one signal pattern, indicating the absence of detectable additional conformers. This behavior could be either related to (a) a fast interconversion among the possible conformers under NMR conditions herein utilized or (b) the presence of a highly predominant more stable conformation. It is also important to mention that the H^{1} NMR temperature of coalescence for thiourea conformers ranges from 0 to 40 °C [26], with our NMR experiments being conducted at 30 °C. Despite of those facts, per-*O*-acylated glycosylthioureas tend to adopt *Z* configuration at the sugar NH–C(═S) bond. Thiourea glycoporphyrin **7** gave a coupling constant of 8.5 Hz, which is in agreement with the expected *anti* relationship for N–H and sugar H-1. This is also in accordance with the relatively shielded anomeric hydrogen (6.04 ppm) presented by **7**. For compound **8**, the coupling constant related to N–H and benzylic hydrogens was 5.3 Hz, this value being more consistent with a *gauche* relative disposition involving the three mentioned hydrogens. Compounds **7** and **8** were then submitted to NOESY ^{1}H–^{1}H NMR experiments. These experiments gave no interactions involving *m*-phenyl hydrogens of the tetra(aryl)pophyrin moiety and the H–N closer to the sugar ring, which excludes the possibility of an *E* conformation. A NOESY cross peak between the two H–N of the thiourea bridge could also be observed. These findings, together with the above-cited literature data, indicated the thiourea bridge as having a *Z,Z* conformation for both **7** and **8**.

Differently, for each of the thiocarbamate derivates (**9** and **11**), two different conformer populations could be observed. Compound

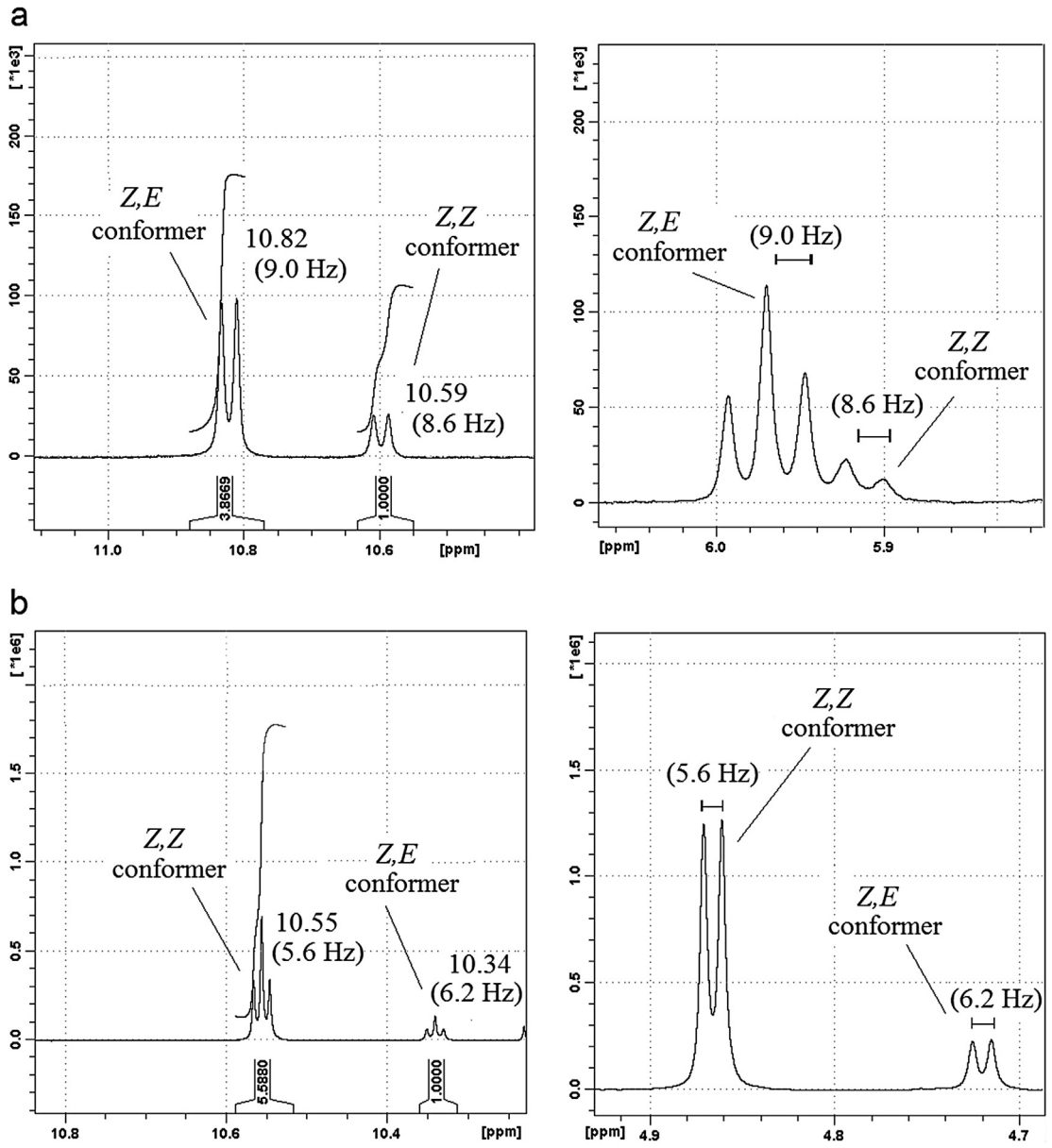

Fig. 1. Selected H^1 NMR signals of H–N and glycosyl-H-1 or benzyl-CH_2 of compounds **9** (a) and **11** (b).

9 had two doublets at 10.82 and 10.59 ppm (integration ratio of 3.9:1, respectively), which were assigned to H–N of the thiocarbamate bridge of the two distinct conformers. These signals had matching coupling constants of 9.0 and 8.6 Hz related to a multiplet (which corresponded to two partially overlapped triplets) attributed to the anomeric hydrogen (H-1) of the glycosyl moiety at 5.97–5.90 ppm (see Fig. 1a). Selective irradiation of H–N of **9** major conformer, at 10.82 ppm, gave NOE peaks at 5.16 and 5.97 ppm (H-2 and H-1 of the sugar moiety, respectively). Together with the characteristic coupling constants, this data suggested that the NH–C(=S) bond had Z configuration. The appearance of another NOE signal at 7.51 ppm (*m*-phenyl hydrogens of the tetra(aryl)pophyrin moiety) defined the thiocarbamate bridge of **9** major conformer as *Z,E*. In turn, **9** minor conformer had only one H–N NOE signal attributed to H-2 of the sugar moiety. The lack of further NOE peaks could be a result of the low abundance of the conformer, which compromised NMR signal gain. Considering chemical shifts and coupling constant values, a minor conformer of **9** should present a *Z,Z* configuration.

^{1}H NMR spectrum of thiocarbamate **11** presented two triplets from H–N (10.55 and 10.34 ppm) and two doublets from benzylic CH_2 (4.86 and 4.71 ppm), also having matching coupling constants of 5.9 and 6.2 Hz, respectively. The ratio between the conformers was higher for thiocarbamate benzyl-porphyrin (5.6:1) than for glycoporphyrin analog (Fig. 1b). The evaluation of the coupling constants allowed us to assign a *Z* conformation between C=S and CH_2 for both conformers. Considering the absence of NOE at 7.52 ppm (*m*-phenyl hydrogens of the tetra(aryl)pophyrin moiety) we could propose a *Z,Z* conformation for the major population of compound **11**. Assuming that compound **11** major and minor conformers should present distinct conformations from each other, we could speculate a *Z,E* conformation for the minor conformer. The lack of an NOE signal involving the *m*-phenyl hydrogens of the tetra(aryl)porphyrin moiety could also be explained by low NMR signal gain, as noticed for compound **9** minor conformer.

It was noteworthy that porphyrin conjugates **9** and **11** were unstable in terms of their thiocarbamate linkages. For example, even storing a DMSO solution of **9** in freezer for only three days, it

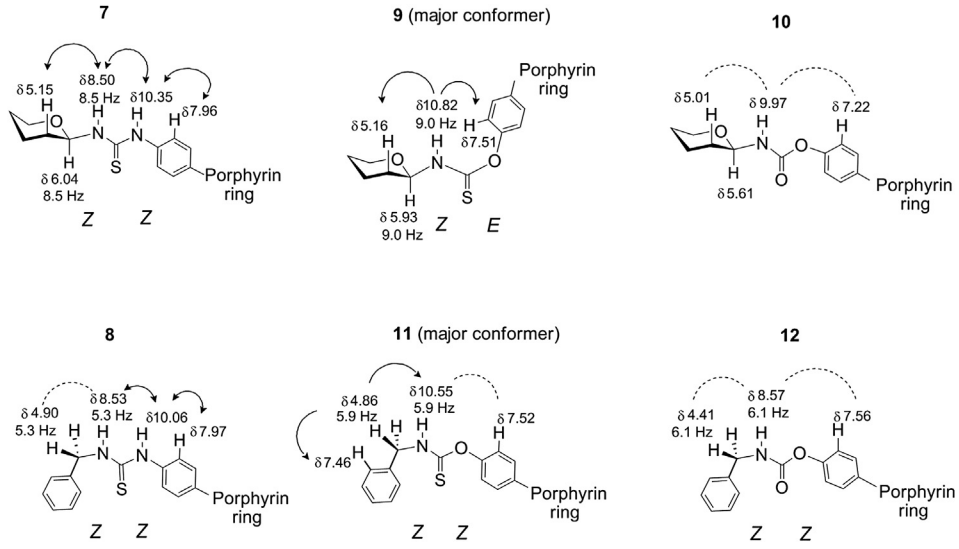

Fig. 2. Most likely conformations of compounds **7**, **8**, **9** (major conformer), **11** (major conformer) and **12**. Key ^{1}H NMR chemical shifts (δ) and coupling constant values (Hz) are shown. One-headed arrows (⟶) represent observed 1D ^{1}H NMR NOE peaks; two-headed arrows (⟷) represent observed 2D ^{1}H–^{1}H NMR NOESY cross peaks and dashed lines (-----) represent non-observed NOE peaks or NOESY cross peaks.

could be noted the appearing of small amounts of porphyrins **4** and **10**. The hydrolysis of the thiocarbamate derivates was somewhat expected because previously studies have already reported this type of behavior under both acid or basic conditions [25]. For this reason, attempts of prolonged or temperature-based NMR experiments, such as NOESY 2D and dynamic ^{1}H NMR, gave disappointingly results due to decomposition during experiment course. In this way, the following physicochemical and photophysical assays were performed using freshly purified **9** and **11** samples.

The carbamate benzyl-porphyrin **12** H–N signal appeared as a triplet (8.57 ppm, $J = 6.1$ Hz) with matching coupling constant with a doublet that corresponded to the benzylic hydrogens (4.41 ppm). The close J value to those observed for the other benzyl-porphyrins (**8** and **11**) indicated that HN–benzyl as having *Z* conformation. The lack of an NOESY cross peak involving H–N and *m*-phenyl hydrogens of the tetra(aryl)pophyrin moiety defined the **12** carbamate bridge with *Z,Z* conformation.

Although carbamate derivative **10** presented mass and ^{13}C NMR spectra compatible to the expected structure, the ^{1}H NMR signals related to the carbamate bridge showed an unexpected multiplicity. Specifically, H–N appeared as a broad signal, while anomeric hydrogen of the glycosyl moiety gave a doublet (it was expected a doublet and a triplet, respectively). All the NMR experiments above-discussed were conducted in deuterated DMSO because this solvent provided proper solubilization for all porphyrin conjugates. We anticipated that specifically for the carbamate bridge of the glycoporphyrin **10**, a substantial H–N hydrogen exchange with the water present in the deuterated solvent could have occurred. This supposition was supported by a presat ^{1}H NMR experiment (water signal suppression using presaturation), which concomitantly eliminated the H–N signal. The expected position and configuration of the O–C(=O)–NH group was confirmed by HMBC ^{1}H–^{13}C NMR that displayed correlations at 5.61/154.4 ppm (H-1/C=O) and 9.97/69.8 ppm (H–N/C-2). Because of the absence of coupling constants, as well as the lack of any NOESY cross peak involving carbamate bridge of **10**, we could not propose any possible conformation for this compound. Fig. 2 present the most likely conformations expected for compounds **7**–**9**, **11** and **12** based on literature data, ^{1}H NMR chemical shifts, coupling constant values and NOE or NOESY experiments (see spectra in Supplementary Information).

3.2. Evaluation of the photophysical and physicochemical properties of porphyrins 7–12

The evaluation of photophysical and physicochemical properties of a PS is current utilized to identify promising molecules for PDT

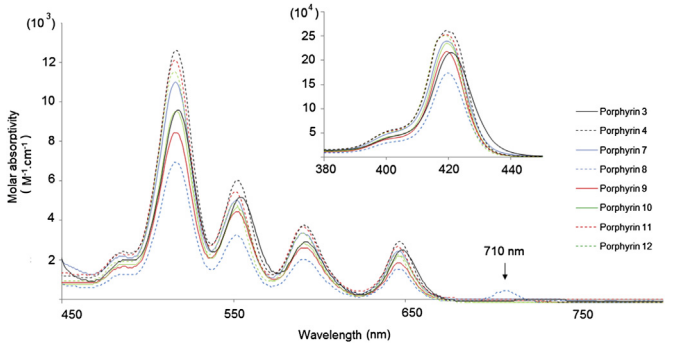

Fig. 3. UV–Vis spectra of Q-bands of porphyrins **7**–**12** at 12 μmol L^{-1} in $CHCl_3$. Inset:Soret band.

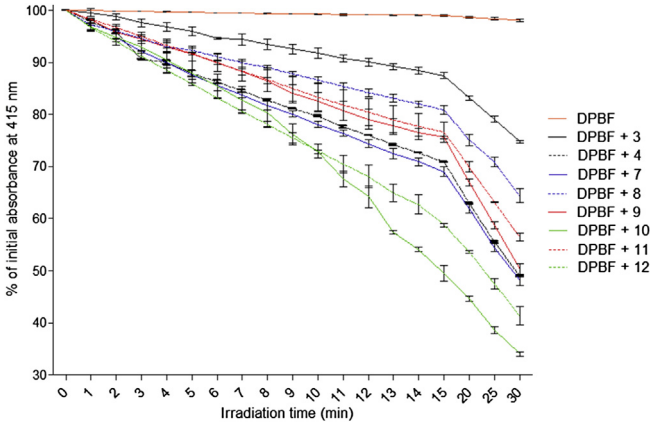

Fig. 4. Singlet oxygen production of **7**–**12**.

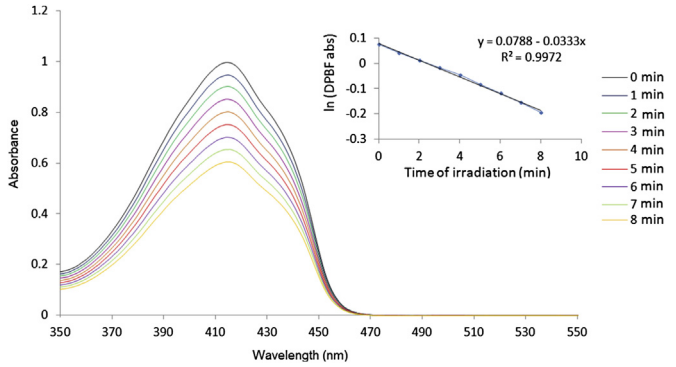

Fig. 5. DPBF consumption in the presence of MB in DMF:H_2O 9:1 at 9 mW/cm^2 (inset: ln (DPBF absorbance) vs irradiation time).

[29,58]. In order to identify whether there was any effect related to the thiourea, thiocarbamate and carbamate bridges on porphyrin electronic spectra, the UV–Vis spectral profile of porphyrins **7**–**12** and synthetic precursors **3** and **4** were recorded. Fig. 3 shows the UV–Vis data for all porphyrins studied. Except for porphyrin **8**, the UV–Vis spectra were very similar for all compounds. For porphyrin **8**, it was found an additional Q-band at a higher wavelength (710 nm). This could be explained by the fact that N–C(=S)–N group shows a preference for polar resonance structures, with the sulfur atom being able to bear a negative charge by making a transitory single bond to the central carbon [26]. In this case, benzylic hydrogens could become more acidic, thus creating the opportunity to extend the aryl-porphyrin group resonance to the benzene ring of the deprotonated benzyl group.

Even though the new band in compound **8** UV–Vis spectrum presented low intensity, we considered this finding important. *Meso*-tetra(aryl)porphyrins have multiple potential sites for placing amino groups, allowing the introduction of additional thiourea bridges. This strategy could be used in the future in order to amplify the absorptivity in the spectral range of 700–850 nm. In such wavelength region, the light shows deeper tissue penetration, which makes possible an increased singlet oxygen production in those tissues and, consequently, increasing PDT efficacy [3,26].

One of the characteristics that are expected from an efficient PS is the ability of generating high amounts of singlet oxygen ($^1O_2$). We estimated $^1O_2$ production for porphyrins **7**–**12** and their synthetic precursors, compounds **3** and **4**, by a previously stated methodology. In this indirect method we measured the decreasing of the absorption of DPBF (1,3-diphenylisobenzofuran) at 415 nm in the presence of the studied porphyrins. We reported the UV–Vis absorption decreasing in terms of percentage from the initial values; thus lower percentages reflect a higher $^1O_2$ production.

Results outlined in Fig. 4 indicated that there was a perceptible correlation between the linker type and the $^1O_2$ production.

Table 3
Singlet oxygen quantum yield (Φ_Δ).

Compound	R	Φ_Δ
Methylene blue	0.0333	0.52
Porphyrin 3	0.0093	0.15 ± 0.051
Porphyrin 4	0.0242	0.38 ± 0.062
Porphyrin 7	0.0234	0.37 ± 0.046
Porphyrin 8	0.0132	0.21 ± 0.053
Porphyrin 9	0.0175	0.27 ± 0.056
Porphyrin 10	0.0295	0.46 ± 0.072
Porphyrin 11	0.0156	0.24 ± 0.067
Porphyrin 12	0.0297	0.46 ± 0.065
Photofrin[a]	–	0.32

[a] Data obtained from Ref. [28].

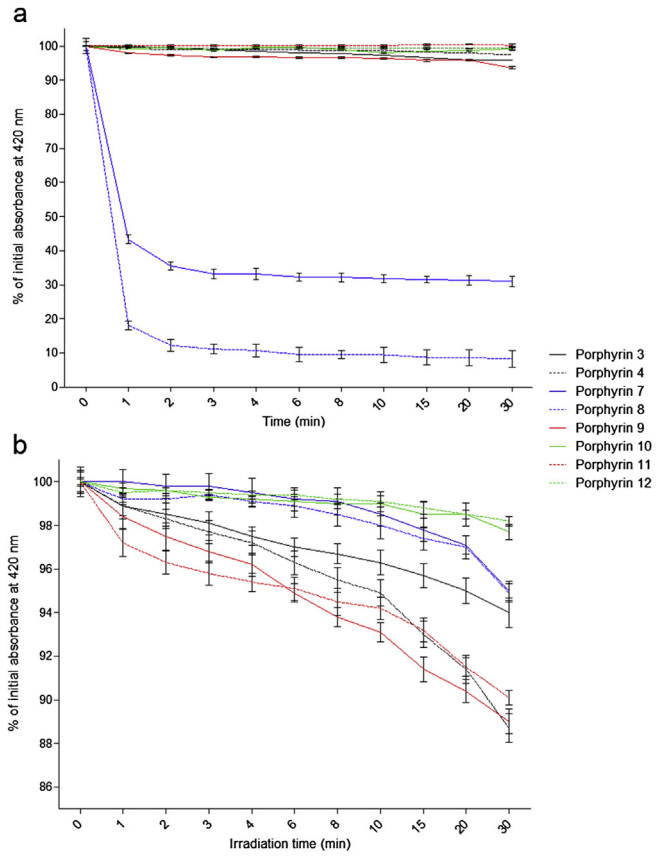

Fig. 6. Photostability study. Porphyrin concentration 10 μM on aqueous media; (a) Soret band extinction in the absence of light on aqueous media. (b) Soret band extinction under irradiation at 100 mW/cm^2; Obs: for graphic (b) **7** and **8** were dissolved in a 0.1 mg% SDS aqueous solution.

Compounds **10** and **12**, both carbamate porphyrin derivates (green lines – Fig. 4), were the best $^1O_2$ producers. Thiourea compounds **7** and **8** gave higher amounts of $^1O_2$ than compound **3** (their synthetic precursor). In turn, thiocarbamate derivates **9** and **11** had close results in comparison to their synthetic precursor (porphyrin **4**).

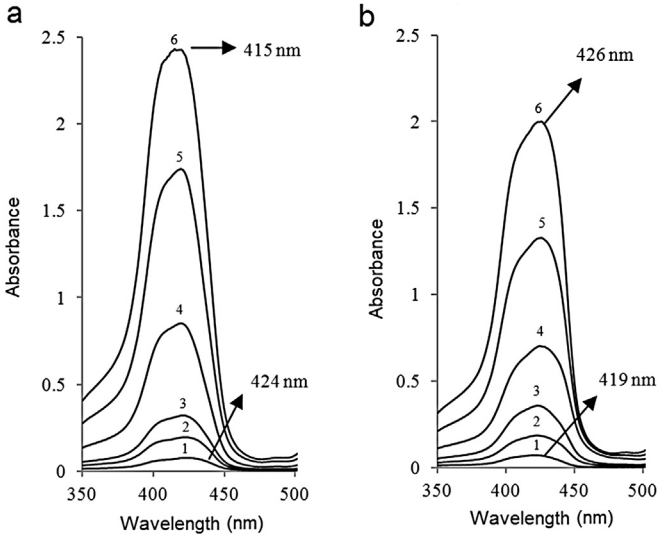

Fig. 7. UV–Vis spectra with different porphyrins concentration. (a)**7** (1) 5 × 10^{-7}; (2) 5 × 10^{-6}; (3) 2 × 10^{-6}; (4) 10^{-6}; (5) 1.5 × 10^{-5}; (6) 10^{-5} mol L^{-1}; (b) **8** (1)1 × 10^{-6}; (2) 5 × 10^{-6}; (3) 2 × 10^{-6}; (4) 2.5 × 10^{-5}; (5) 1.5 × 10^{-5}; (6) 10^{-5} mol L^{-1}.

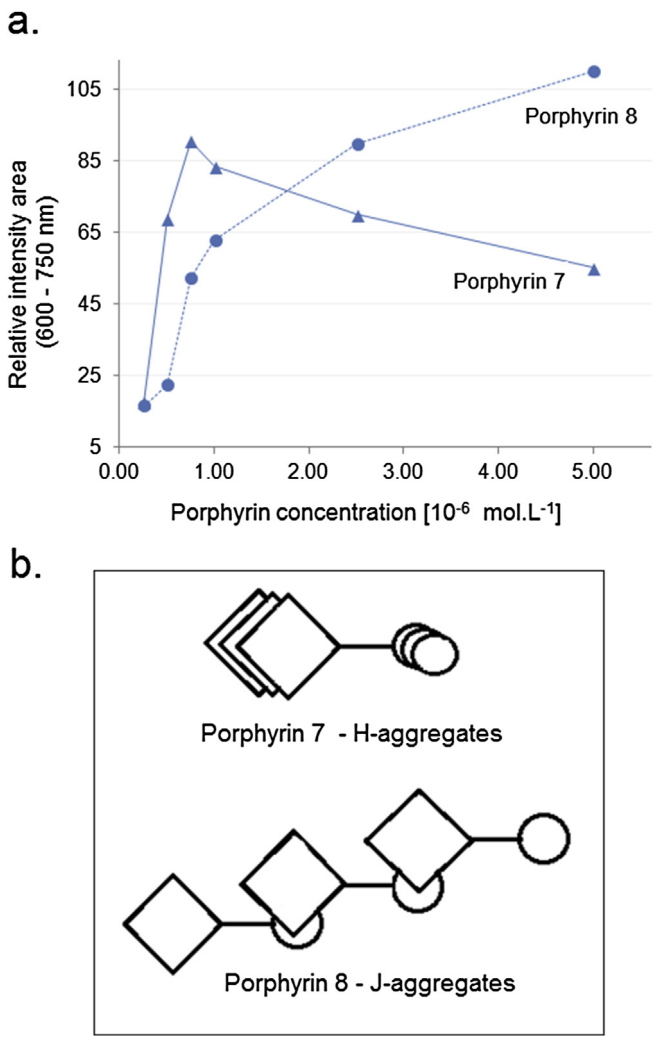

Fig. 8. (a) Changes in fluorescence emission spectra. Plot of relative intensity area from 660 to 750 nm over concentration of **7** and **8** in aqueous solution. Circles and triangles represent the experimental data points. (b) The proposed H- and J-aggregation structure of the porphyrins **7** and **8**. Squares = porphyrin ring; lines = linker; circles = benzyl or glycosyl moiety.

Porphyrin $^1O_2$ quantum yields (Φ_Δ), were determined with MB as standard photosensitizer, as previously stated [29]. By plotting ln of DPBF absorbance during irradiation time in the presence of MB, we were able to extract the angular coefficient, which was named as the standard rate constant of DPBF consumption (R^{Std}) (Fig. 5). The same procedure was also performed for each of the studied porphyrins to give their individual rate constant of DPBF consumption (R). From Equation (1), we then calculated the singlet oxygen quantum yields, as shown in Table 3. These results indicated that the carbamate derivates **10** and **12** gave the highest $^1O_2$ production ($\Phi_\Delta = 0.46$) among the tested porphyrins, which confirmed the experiments outlined in Fig. 4. The comparison of the data found in the present study and the value of Φ_Δ for Photofrin® ($\Phi_\Delta = 0.32$) [28] make compounds **10** and **12** good candidates as photosensitizer for PDT treatments.

The photodynamic action of porphyrins also depends on the integrity of the macrocyclic ring during light irradiation. The photostability study of porphyrins **7**–**12** and compounds **3** and **4** was performed by measuring the Soret band extinction in aqueous media. Because many factors could influence the decrease of the Soret band, such as aggregation and chemical degradation, we first evaluated the behavior of the porphyrins in the absence of light. As shown in Fig. 6a, in a preliminary study we could observe that **7** and **8** had an intense decreasing of the Soret band absorption in the first 3 min. This behavior was compatible with events of molecular aggregation. To avoid the impact of aggregation during photostability studies, we first developed a surfactant system that did not cause a significant interference on Soret band absorption. This consisted of a diluted solution of SDS 0.1 mg/100 mL. In this way, compounds **7** and **9** were submitted to the photostability test being dissolved in the SDS solution instead of water. As observed for the $^1O_2$ production study, we found an important correlation between the linkage and the photostability results. Thiocarbamate porphyrins derivates **9** and **11** were the less photostable compounds, presenting a Soret band extinction profile very similar to their synthetic precursor (compound **4**). Thiourea derivatives **7** and **8** were more photostable than their synthetic precursor (porphyrin **3**), with the carbamates **10** and **12** being the most photostable compounds in the study (Fig. 6b).

Both **7** and **8** thiourea porphyrin conjugates aggregated in aqueous media. We then wondered if their self-assembling properties were equal, as they were closely related compounds. So, we evaluated them by UV–Vis (Fig. 7) and fluorescence spectroscopy (Fig. 8a) through a previously stated method based on the exciton theory established by Kasha and coworkers [38,59,60]. According to this theory, the shifts in UV–Vis spectra and the changes in fluorescence emission intensity can indicate the geometry achieved after self-assembling events. Surprisingly, the aggregation properties were not the same for the thiourea conjugates. Whilst increasing the concentration of porphyrin **7** resulted in a blue-shift of the Soret band, porphyrin **8** showed a red-shifting behavior. In agreement with the UV–Vis experiment, concentration increase produced a decrease in the fluorescence intensity for **7** and a fluorescence enhancement for **8**. This is consistent with the formation of H-aggregates for porphyrin **7** and J-type aggregates for porphyrin **8**, respectively. The appearance of a shoulder band and a relatively broad profile at half-height indicated that only part of the porphyrins in the solution became H- or J-aggregates and, thereby, porphyrin monomers are still present, even under high porphyrin concentration. With these results we were able to propose a geometry arrangement for the aggregates of glycoporphyrin **7** and benzyl-porphyrin **8**, as shown on Fig. 8b.

4. Conclusions

Here, we described the synthesis of glyco- and benzyl-tetra(aryl)porphyrin conjugates (**7**–**12**) bearing thiourea, thiocarbamate or carbamate linkers from monosubstituted amino- (**3**) or hydroxy- (**4**) *meso*-tetra(aryl)porphyrins and per-*O*-acetyl-β-D-glucopyranosyl **5** or benzyl isothiocyanates **6**. Glycoporphyrins could be obtained in better yields than their respective non-glycosyl analogs. Thiourea conjugates were obtained in higher yields in comparison to the thiocarbamate and carbamate compounds. An ultrasound-assisted method was successfully executed for the preparation of those glycoporphyrins having thiourea and carbamate bridges with a drastic reduction of the reaction time. Benzyl-porphyrins could not be prepared by the ultrasound protocol. Attempts to define bridge conformation suggested that thiourea and carbamate linkers tend to appear as *Z,Z* conformers. Thiocarbamate derivatives presented distinct populations of detectable rotamers, which were detected by using NMR spectroscopy. Major conformer of the glycoporphyrin thiocarbamate was assigned as *Z,E*. We also observed a high correlation between the type of linker and photophysical properties that allowed us to identify the carbamate porphyrin derivates as the most promising photosensitizers among the studied molecules. Carbamate

derivatives showed a high singlet oxygen production and good photostability, with no self-assembling behavior in aqueous media. Based on these results, the synthesis of new porphyrin conjugates that combine the best structural features herein determined can be performed. The investigation of the photodynamic biological activity of these compounds is currently under investigation in our laboratories.

Acknowledgments

This work was supported by grants from Fundação Araucária (15152), CAPES and PRONEX-Carboidratos (14669). J.C.C.D. thanks the scholarship from CNPq (National Research Council of Brazil). M.E.D and M.D.N are research members of CNPq. A. G. G. is a research member of Fundação Araucária. The authors are thankful to Professor Luciano Huergo and Dr. Lauro M. Souza for high resolution mass spectroscopy, to Professor Guilherme Sassaki from UFPR NRM Center for NOE and NOESY NMR experiments and to UFPR Vibrational Spectroscopy Laboratory for FTIR experiments.

Appendix A. Supplementary data

Supplementary data related to this article can be found at http://dx.doi.org/10.1016/j.dyepig.2014.03.029.

References

[1] Brown SB, Brown EA, Walker I. The present and future role of photodynamic therapy in cancer treatment. Lancet Oncol 2004;5:497–508.
[2] Bonnett R. Photodynamic therapy in historical perspective. Rev Contemp Pharm 1999;10:1–17.
[3] O'Connor AE, Gallagher WM, Byrne AT. Porphyrin and nonporphyrin photosensitizers in oncology: preclinical and clinical advances in photodynamic therapy. Photochem Photobiol 2009;85:1053–74.
[4] Sanabria LM, Rodríguez ME, Cogno IS, Belén N, Vittar R, Pansa MF, et al. Direct and indirect photodynamic therapy effects on the cellular and molecular components of the tumor microenvironment. Biochim Biophys Acta 2013;1835:36–45.
[5] Castano AP, Demidova TN, Hamblin MR. Mechanisms in photodynamic therapy: part two – cellular signaling, cell metabolism and modes of cell death. Photodiag Photodyn 2005;2:1–23.
[6] Yano S, Hirohara S, Obata M, Hagiya Y, Ogura S, Ikeda A, et al. Current states and future views in photodynamic therapy. J Photochem Photobiol C Photochem Rev 2011;12:46–67.
[7] Kejík Z, Bříza T, Králová J, Poučková P, Král A, Martásek P, et al. Coordination conjugates of therapeutic proteins with drug carriers: a new approach for versatile advanced drug delivery. Bioorg Med Chem Lett 2011;21:5514–20.
[8] Umezawa N, Matsumoto N, Iwama S, Kato N, Higuchi T. Facile synthesis of peptide-porphyrin conjugates: towards artificial catalase. Bioorg Med Chem 2010;18:6340–50.
[9] James DA, Swamy N, Paz N, Hanson RN, Ray R. Synthesis and estrogen receptor binding affinity of a porphyrin-estradiol conjugate for targeted photodynamic therapy of cancer. Bioorg Med Chem Lett 1999;9:2379–84.
[10] Ethirajan M, Chen Y, Joshi P, Pandey RK. The role of porphyrin chemistry in tumor imaging and photodynamic therapy. Chem Soc Rev 2011;40:340–62.
[11] Zheng X, Pandey RK. Porphyrin-carbohydrate conjugates: impact of carbohydrate moieties in photodynamic therapy (PDT). Anticancer Agents Med Chem 2008;8:241–68.
[12] Jain K, Kesharwani P, Gupta U, Jain NK. A review of glycosylated carriers for drug delivery. Biomaterials 2012;33:4166–86.
[13] Rambaruth NDS, Dwek MV. Cell surface glycan-lectin interactions in tumor metastasis. Acta Histochem 2011;113:591–600.
[14] Vlodavsky Sachs L. Lectin receptors on the cell surface membrane and the kinetics of lectin-induced cell agglutination. Exp Cell Res 1975;93:111–9.
[15] Aicher D, Wiehe A, Stark C. Synthesis of glycoporphyrins using trichloroacetimidates as glycosyl donors. Synlett 2010;2010:395–8.
[16] Laville I, Figueiredo T, Loock B, Pigaglio S, Maillard P, Grierson D, et al. Synthesis, cellular internalization and photodynamic activity of glucoconjugated derivatives of tri and tetra(meta-hydroxyphenyl)chlorins. Bioorg Med Chem 2003;11:1643–52.
[17] Tomé JPC, Silva EMP, Pereira AMVM, Alonso CMA, Faustino MAF, Neves MGPMS, et al. Synthesis of neutral and cationic tripyridylporphyrin-D-galactose conjugates and the photoinactivation of HSV-1. Bioorg Med Chem 2007;15:4705–13.
[18] Garcia G, Naud-Martin D, Carrez D, Croisy A, Maillard P. Microwave-mediated "click-chemistry" synthesis of glycoporphyrin derivatives and in vitro photocytotoxicity for application in photodynamic therapy. Tetrahedron 2011;67:4924–32.
[19] Locos OB, Heindl CC, Corral A, Senge MO, Scanlan EM. Efficient synthesis of glycoporphyrins by microwave-mediated "Click" reactions. Eur J Org Chem 2010;2010:1026–8.
[20] Laville I, Pigaglio S, Blais JC, Loock B, Maillard P, Grierson D, et al. A study of the stability of tri(glucosyloxyphenyl)chlorin, a sensitizer for photodynamic therapy, in human colon tumoral cell: a liquid chromatography and MALDI-TOF mass spectrometry analysis. Bioorg Med Chem 2004;12:3673–82.
[21] Lafont D, Zorlu Y, Savoie H, Albrieux F, Ahsen V, Boyle RW, et al. Monoglycoconjugated phthalocyanines: effect of sugar and linkage on photodynamic activity. Photodiag Photodyn 2013;10:252–9.
[22] Hermanson GT. Bioconjugate techiniques. 2nd ed. London: Elsevier Inc.; 2008.
[23] Clarke OJ, Boyle RW. Isothiocyanatoporphyrins, useful intermediates for the conjugation of porphyrins with biomolecules and solid supports. Chem Commun 1999;1999:2231–2.
[24] Rusin O, Hub M, Král V. Novel water-soluble porphyrin-based receptors for saccharide recognition. Mater Sci Eng C 2001;18:135–40.
[25] Humeres E, de Souza EP, Debacher NA. The mechanisms of hydrolysis of N-alkyl O-arylthioncarbamate esters. J Phys Org Chem 2010;23:915–24.
[26] Garcia Fernández JM, Ortiz Mellet C. Chemistry and developments of N-thiocarbonyl carbohydrate derivatives: sugar isothiocyanates, thioamides, thioureas, thiocarbamates, and their conjugates. Adv Carbohydr Chem Biochem 2000;55:35–135.
[27] Guo L, Yan B. Near-infrared luminescent hybrid materials using modified functional lanthanide (Nd3+, Yb3+) porphyrins complexes chemical bonded with silica. Inorg Chem Commun 2011;14:1833–7.
[28] Silva P, Fonseca SM, Arranja CT, Burrows HD, Urbano AM, Sobral AJFN. A new nonconjugated naphthalene derivative of meso-tetra-(3-hydroxy)-phenylporphyrin as a potential sensitizer for photodynamic therapy. Photochem Photobiol 2010;86:1147–53.
[29] de Assis FF, de Souza JM, Assis BHK, Brocksom TJ, de Oliveira KT. Synthesis and photophysical studies of a chlorin sterically designed to prevent self-aggregation. Dyes Pigment 2013;98:153–9.
[30] Armarego WLF, Perrin DD. Purification of laboratory chemicals. 4th ed. Oxford: Butterworth-Heinemann; 2000.
[31] Kruper WJ, Chamberlim TA, Kachanny M. Regiospecific aryl nitration of meso-substituted tetraarylporphyrins: a simple route to bifunctional porphyrins. J Org Chem 1989;54:2753–6.
[32] Kumar D, Shekar KPC, Mishra B, Kumar A, Akamatsu K, Kusaka E, et al. A facile synthesis and cytotoxicity of novel porphyrin-cryptolepine conjugates. Chem Biol Interface 2012;2:114–21.
[33] Tomé JPC, Neves MGPMS, Tomé AC, Cavaleiro JAS, Mendonça AF, Pegado IN, et al. Synthesis of glycoporphyrin derivatives and their antiviral activity against herpes simplex virus types 1 and 2. Bioorg Med Chem 2005;13:3878–88.
[34] Camarasa JM, Fernadez-Reza P, Garcia-Lopez TM, Heras, frederico G, Mendez-Castrillon PP, Felix AS. A new procedure for the synthesis of glycosyl isothiocyanates. Synthesis 1984;1984:509–10.
[35] Kitamura T, Kobayashi S, Taniguchi H. Photolysis of vinyl halides. Reaction of photogenerated vinyl cations with cyanate and thiocyanate ions. J Org Chem 1990;55:1801–5.
[36] Roitman L, Ehrenperb B, Kabayashi N. Spectral properties and absolute determination of singlet oxygen production by naphthaloporphyrins. J Photochem Photobiol A Chem 1994;77:23–8.
[37] Gomes MC, Barreira SMW, Faustino MAF, Fernandes R, Neves MG, Tomé AC, et al. Photodynamic inactivation of *Penicillium chrysogenum* conidia by cationic porphyrins. Photochem Photobiol Sci 2011;10:1735.
[38] Guo L. Side-chain-controlled H- and J-aggregation of amphiphilic porphyrins in CTAB micelles. J Colloid Interface Sci 2008;322:281–6.
[39] Lee C-H, Lindsey JS. One-flask synthesis of meso-substituted dipyrromethanes and their application in the synthesis of trans-substituted porphyrin building blocks. Tetrahedron 1994;50:11427–40.
[40] Ló SMS, Ducatti DRB, Duarte MER, Barreira SMW, Noseda MD, Gonçalves AG. Synthesis of *meso*-tetraarylporphyrins using SeO_2 as oxidant. Tetrahedron Lett 2011;52:1441–3.
[41] Osati S, Safari N, Jamaat PR. Synthesis and characterization of three covalently linked porphyrin-phthalocyanine pentamers with nucleophilic substitution. Inorg Chim Acta 2010;363:2180–4.
[42] Durantini EN, Silber JJ. Synthesis of 5-(4-acetamidophenyl)-10,15,20-tris(4-substituted phenyl)porphyrins using dipyrromethanes. Synth Commun 1999;29:3353–68.
[43] Monti D, Venanzi M, Mancini G, Marotti F, La Monica L, Boschi T. Synthesis and complexation properties of an oligooxaethylene-spacered porphyrin dimer – toward the construction of a new switchable porphyrin array. Eur J Org Chem 1999;1999:1901–6.
[44] Kuhne M, Gyorgydeak Z, Lindhorst TK. A simple method for the preparation of glycosyl isothiocyanates. Synthesis 2006;6:949–51.
[45] Jimenez Blanco J, Sylla B, Ortiz Mellet C, Garcia Fernandez JM. Synthesis of alfa and beta-glycosyl isothiocyanates via oxazoline intermediates. J Org Chem 2007;72:4547–50.
[46] Lindhorst TK, Kieburg C. Solvent-free preparation of glycosyl isothiocyanates. Synthesis; 1995:1228–30.
[47] L'abbé G, Leurs S, Sannen I, Dehaen W. Synthesis of thiazolo [4,3-a]isoindoles by intramolecular cycloaddition-elimination reactions of 4-methyl-5-(substituted)imino-1,2,3,4-thiatriazolines. Tetrahedron 1993;49:4439–46.

[48] Falconer RA, Toth I. Design, synthesis and biological evaluation of novel lipoamino acid-based glycolipids for oral drug delivery. Bioorg Med Chem 2007;15:7012–20.
[49] Prata C, Mora N, Lacombe JM, Maurizis JC, Pucci B. Synthesis and surface-active properties of glycosyl carbamates and thioureas. Carbohydr Res 1999;321:4–14.
[50] Zhou Y, Wang L, Han L, Meng F, Yang C. Synthesis, antifungal activities, and potential detoxification of N-(2,3,4,6-tetra-O-acetyl-beta-D-glucopyranosyl) thiocarbamates. Carbohydr Res 2009;344:1289–96.
[51] Joshi UM, Patkar LN, Rajappa S. Concomitant desulfurization and transesterification of alkyl thionocarbamates. Synth Commun 2004;34:33–9.
[52] Viana GM, Aguiar LC de S, Ferrão J de A, Simas ABC, Vasconcelos MG. The use of aqueous potassium dichloroiodate for the synthesis of ureas. Tetrahedron Lett 2013;54:936–40.
[53] Ichikawa Y, Nishiyama T, Isobe M. Stereospecific synthesis of urea-tethered neoglycoconjugates starting from glucopyranosyl carbamates. Tetrahedron 2004;60:2621–7.
[54] Ichikawa Y, Ohara F, Kotsuki H, Nakano K. A new approach to the neoglycopeptides: synthesis of urea and carbamate-tethered N-acetyl-D-glucosamine amino acid conjugates. Org Lett 2006;8:5009–12.
[55] Sansone F, Chierici E, Casnati A, Ungaro R. Thiourea-linked upper rim calix[4]arene neoglycoconjugates: synthesis, conformations and binding properties. Org Biomol Chem 2003;1:1802–9.
[56] Paizs B, Pinter I, Csizmadia IG. An exploratory study of 1,2-cis- and 1,2-trans-thiocarbamates of glucofuranosyl- and glucopyranosylamine. J Mol Struct Theochem 1998;455:267–74.
[57] Plutín AM, Suárez M, Ochoa E, Machado T, Mocelo R, Concellón JM, et al. Synthesis of new acyl, furoyl, and benzoylthiocarbamates as polydentate systems. Structural study of isopropyl N-(2-furoyl)thiocarbamate. Tetrahedron 2005;61:5812–7.
[58] Bautista-Sanchez A, Kasselouri A, Desroches MC, Blais J, Maillard P, Oliveira DM, et al. Photophysical properties of glucoconjugated chlorins and porphyrins and their association with cyclodextrins. J Photochem Photobiol B Biol 2005;81:154–62.
[59] Kasha M, Rawls HR, El-Bayoumi MA. The exciton model in molecular spectroscopy. Pure Appl Chem 1965;11:371–92.
[60] Ali M, Pandey S. Aggregation behavior of aqueous tetrakis(4-sulfonatophenyl) porphyrin in the presence of 1-butyl-3-methylimidazolium tetrafluoroborate. J Photochem Photobiol A Chem 2009;207:288–96.